Morphometric and anatomic study of the hind limb of a dog

Ron Shahar, DVM, and Joshua Milgram, DVM

Objective—To obtain the anatomic and morphometric data required for biomechanical analysis of the hind limb in dogs.

Animals—A healthy adult mixed-breed 23-kg male dog.

Procedure—Following euthanasia of the dog, all muscles of the right hind limb were identified and meticulously removed. Physiologic cross-sectional areas (PCSA) and architectural indices (AI) were calculated. The coordinates for the origin and insertion of each muscle were determined, using orthogonal right-handed coordinate systems embedded in the pelvis, femur, and tibia.

Results—PCSA and AI were calculated for 29 muscles, and coordinates for the origins and insertions of these muscles were determined.

Conclusions—Results provide the morphometric and anatomic data necessary for 3-dimensional biomechanical studies of the hind limb in dogs. (*Am J Vet Res* 2001;62:928–933)

Three-dimensional biomechanical analysis of the hind limb requires knowledge of the magnitudes and directions of all forces acting on the limb.[1-13] These forces include the joint reaction forces and moments and the forces in all the muscles that surround the joints of the limb. Forces transmitted by joints and associated periarticular structures and muscle forces are difficult to determine directly through in vivo measurements.[3-6,8,13] Therefore, an indirect approach is typically used to determine these forces and moments. Such an approach is based on modeling the hind limb as a system of rigid bodies connected at the joints. Forces and moments acting on these bodies are then determined by solving the equations governing their equilibrium.

Formulating and solving these equations requires some basic morphometric and anatomic data concerning the **physiologic cross-sectional area (PCSA)**, **architectural index (AI)**, and angle of pennation of each muscle and the location of each muscle's origin and insertion. The PCSA of a muscle represents the ratio of muscle volume to effective muscle fiber length.[14] It reflects the number of sarcomeres in parallel in that muscle and is, therefore, proportional to the amount of force the muscle can generate. The AI of a muscle, on the other hand, reflects the number of sarcomeres in series in that muscle and is, therefore, proportional to the potential velocity of muscle contraction. Values for the PCSA of the muscles of the lower limb in humans,[6,14] the hind limb in cats,[15] and the forelimb in chimpanzees[16] have been published. To our knowledge, however, information regarding the PCSA of the muscles of the hind limb in dogs has not been.

Formulation of these equations of equilibrium also requires knowledge of the direction of force in each muscle and its moment arm around the joint on which it has an effect. A common method of determining the direction of force in a muscle is the straight line model.[5,7,9,17,18] This model assumes that the force generated by a muscle acts along the straight line that connects the origin and insertion of that muscle. The moment arm of a muscle about a joint is the vector connecting the muscle's point of insertion to the joint center.[1-5,7,9,10,13,18] Therefore, biomechanical analysis of the hind limb requires information on the locations of the origins and insertions of all muscles that affect the joints of the hind limb, as well as the locations of all joint centers.

The purpose of the study reported here was to obtain the anatomic and morphometric data required for biomechanical analysis of the hind limb in dogs. This included determining the PCSA, AI, and angle of pennation for all muscles of the hind limb, the coordinates of the origins and insertions of those muscles, and the coordinates of bony landmarks that would allow determination of the locations of the centers of the joints of the hind limb.

Materials and Methods

Morphometric variables—An adult mixed-breed 23-kg male dog was used. The dog had been euthanatized at a local pound because of dog population control regulations; it had been healthy at the time of euthanasia. Immediately after the dog was euthanatized, the skin and subcutaneous tissues of the hindquarters were carefully removed. All muscles of the right hind limb were identified and meticulously removed, taking care to preserve all muscle tissue. Muscles that had both their origin and insertion in the tibial-tarsal-metatarsal unit were discarded, because the model used in this study considered this unit to be rigidly connected, eliminating the effect of these muscles. All tendinous tissue was discarded, and muscles were weighed. The following muscles were evaluated: gluteus superficialis muscle, gluteus medius muscle, gluteus profundus muscle, piriformis muscle, cranial portion of the tensor fasciae latae muscle, caudal portion of the tensor fasciae latae muscle, cranial portion of the sartorius muscle, caudal portion of the sartorius muscle, rectus femoris muscle, biceps femoris muscle, abductor cruris caudalis muscle, semimembranosus muscle, semitendinosus muscle, gracilis muscle, adductor longus muscle, adductor magnus et brevis muscle, pectineus muscle, obturatorius internus muscle, obturatorius externus muscle, gemelli muscle, quadratus femoris muscle, articularis coxae muscle, iliopsoas muscle, vastus lateralis muscle, vastus intermedius muscle, vastus medialis muscle, popliteus muscle, extensor digitorum longus muscle, medial head of the gastrocnemius muscle,

Received Apr 18, 2000.
Accepted Jun 26, 2000.
From the Section of Surgery, Koret School of Veterinary Medicine, Hebrew University of Jerusalem, Jerusalem, Israel.

and lateral head of the gastrocnemius muscle. Because the vastus lateralis and vastus intermedius muscles could not be easily and consistently separated, they were considered a single unit. The tensor fasciae latae and sartorius muscles were separated into cranial and caudal parts. The gastrocnemius muscle was considered as 2 separate muscles, because its 2 heads have distinct origins, although they have a common insertion. Distal separation of the 2 heads was assisted by the distinct fiber orientation of each head. Each muscle was weighed with an electronic digital scale. Measurement precision was ± 0.01 g.

Total length of each muscle and its angle of pennation were measured immediately after weighing. Each muscle was placed on a flat dissection surface, and its length was measured with a flexible tape measure. Measurement precision was ± 0.05 cm. Total length of the muscle was subjectively defined as the overall distance between its tendinous attachments.[19,20] The angle of pennation for each muscle was evaluated with a protractor. It varied between 0 and 18° and was < 5° for most muscles. Because the angle of pennation becomes a significant factor in the calculation of PCSA only for angles > 20°,[16] these data were considered to be of minor importance and were discarded.

Fiber length was determined as described.[15] Briefly, each muscle was placed in neutral-buffered 10% formalin for 48 to 72 hours. It was then soaked in 0.4*M* phosphate-buffered saline solution, pH 7.2, for 24 to 48 hours and then placed in 20% sulfuric acid solution for 3 to 7 days until bundles of fibers could be teased apart easily. A small bundle of fibers was dissected from the muscle, using surgical forceps, and the length of the bundle was measured with a flexible tape measure. If fiber length appeared to be nonuniform, several representative bundles were measured, and mean length was calculated. Measurement precision was ± 0.05 cm.

The PCSA was calculated as $(m \bullet \cos \alpha)/(l \bullet \rho)$, where m is the muscle mass (g), α is the average angle of pennation for the muscle fibers, l is the muscle fiber length (cm), and ρ is the muscle tissue density. For this study, muscle tissue den-

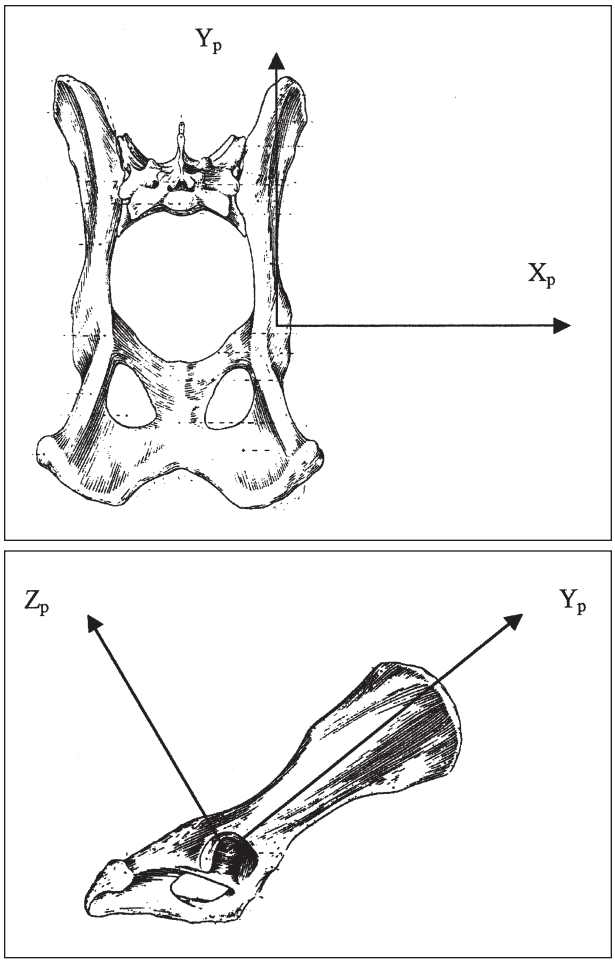

Figure 1—Dorsal (top) and lateral (bottom) views of the pelvis of a dog illustrating the right-handed orthogonal coordinate system.

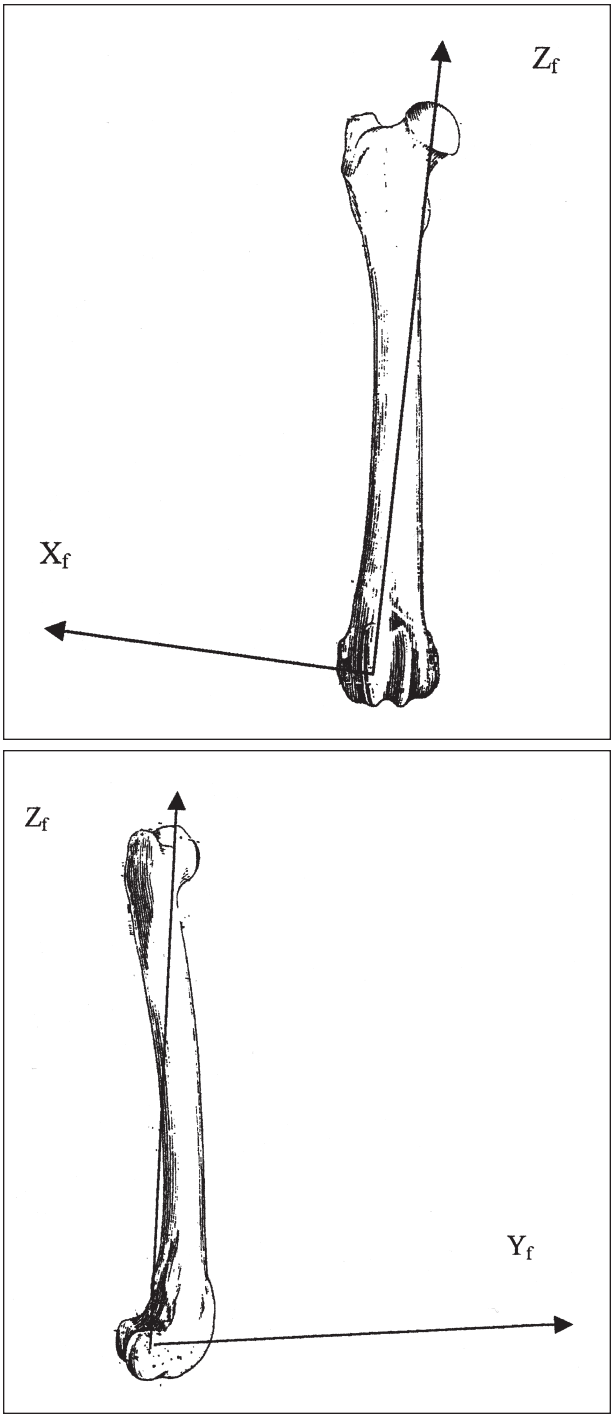

Figure 2—Cranial (top) and lateral (bottom) views of the right femur of a dog illustrating the right-handed orthogonal coordinate system.

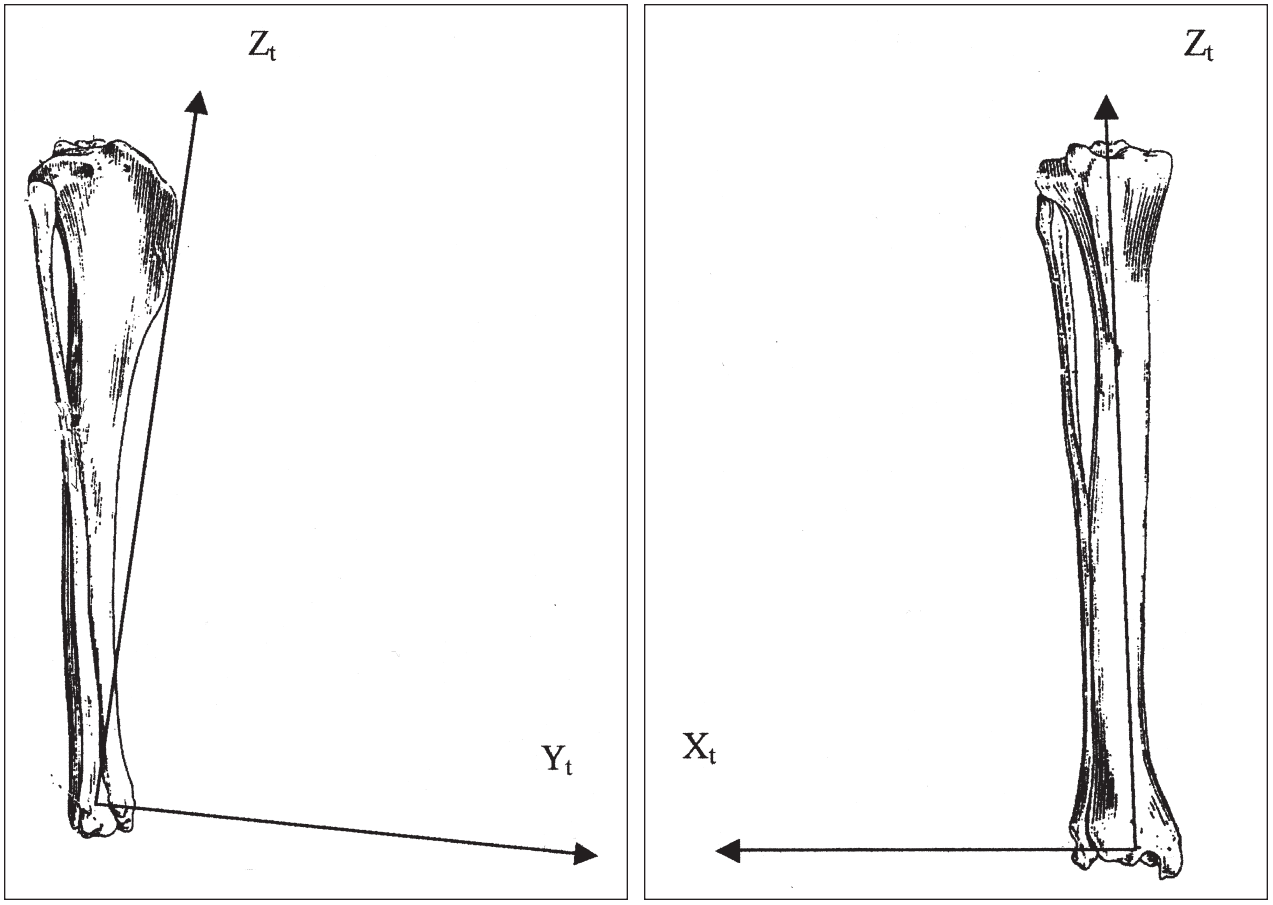

Figure 3—Cranial (right) and lateral (left) views of the right tibia of a dog illustrating the right-handed orthogonal coordinate system.

Table 1—Morphometric data for the muscles of the right hind limb in a dog

Muscle	Muscle mass (g)	Total muscle length (cm)	Muscle fiber length (cm)	PCSA (cm^2)
Gluteus superficialis	21.39	6.9	3.8	5.32
Gluteus medius	79.27	9.1	3.5	21.39
Gluteus profundus	8.97	11.7	1.6	5.29
Piriformis	8.29	5.2	1.8	4.35
Tensor fasciae latae, cranial part	28.88	8.9	2.0	13.64
Tensor fasciae latae, caudal part	6.79	3.6	3.0	2.14
Sartorius, cranial part	33.65	16.3	11.5	2.76
Sartorius, caudal part	19.69	21.0	18.0	1.18
Rectus femoris	49.00	14.1	2.5	18.51
Biceps femoris	181.15	16.7	6.0	28.51
Abductor cruris caudalis	3.80	20.4	15.1	0.24
Semimembranosus	133.86	14.2	12.5	10.99
Semitendinosus	62.32	15.0	13.1	5.77
Gracilis	63.43	10.0	6.6	9.08
Adductor longus	10.02	6.0	2.5	2.87
Adductor magnus et brevis	137.50	13.5	9.1	14.27
Pectineus	12.70	6.3	1.5	7.99
Obturatorius internus	12.47	4.8	1.5	7.85
Obturatorius externus	11.74	4.8	2.0	5.54
Gemelli	2.04	3.2	0.9	2.14
Quadratus femoris	8.30	4.6	2.9	2.70
Articularis coxae	0.49	2.5	1.9	0.24
Iliopsoas	44.84	17.0	6.7	6.32
Vastus lateralis and intermedius	109.75	13.8	5.1	20.32
Vastus medialis	61.23	12.4	2.7	21.41
Extensor digitorum longus	17.26	11.8	2.4	6.79
Gastrocnemius, medial head	28.01	10.5	1.3	20.35
Gastrocnemius, lateral head	29.34	11.8	1.1	25.19
Popliteus	6.84	6.1	1.3	4.97

Values were determined by means of dissection of a healthy adult 23-kg crossbred male dog.
PCSA = Physiologic cross-sectional area.

sity was assumed to be 1.059 g • cm^{-3}.[21] The AI of the muscle was calculated as I/L, where L is the total muscle length (cm).

Anatomic variables—Anatomic preparations of the pelvis and right femur, tibia, and tarsus-metatarsus used for determination of morphometric data were prepared and dried. Points representing the centers of muscle attachment were marked on these preparations. The locations of the points representing the origin and insertion of each muscle were determined on the basis of results of muscle dissection and a standard anatomy textbook.[22] Several additional points representing prominent bony landmarks were also marked. The tarsus and metatarsus were rigidly connected to the tibia so that the long axis of the tibia formed a 130° angle with the long axis of the metatarsus, which is within the reported range of the angle of the hock in standing dogs.[23,24]

Coordinates of points representing muscle attachments and bony landmarks were determined with an electronic coordinate measuring device.[a] Measurement precision was ± 0.001 mm. Bony landmarks in the pelvis, right femur, and right tibia were selected to allow creation of right-handed orthogonal coordinate systems embedded in each bone, with the axes approximately

coinciding with clinical directions (cranial-caudal, medial-lateral, and ventral-dorsal).[25] These bony landmarks were selected on the basis of ease of identification on radiographs and were chosen so that the coordinates of muscle origins and insertions in other dogs could be determined by means of anthropometric scaling of data from radiographs.[26,27]

The origin of the pelvic coordinate system was set at the center of the right acetabulum (**Fig 1**). The Y_p axis was parallel to a line connecting the pubic tubercle and the midpoint between the right and left caudal ventral iliac spines and was directed, therefore, in an approximately cranial direction. The Z_p axis was set perpendicular to the plane defined by the left and right caudal ventral iliac spines and the pubic tubercle and was directed in an approximately dorsal direction. The X_p axis was defined as the vector cross product of the Y_p and Z_p axis and was directed in an approximately lateral direction.

The origin of the femoral coordinate system was set at the midpoint between the medial and lateral epicondyles of the right femur (**Fig 2**). The Z_f axis was defined as the line connecting the origin with the center of the femoral head and approximated the direction of the femoral diaphysis. The Y_f axis was defined as the vector cross product of the Z_f axis and the line connecting the origin and the lateral epicondyle and approximated the cranial direction. The X_f axis was defined as the vector cross product of the Y_f and Z_f axes and approximated a lateral direction.

The origin of the tibial coordinate system was set at the midpoint between the medial and lateral malleoli of the right tibia (**Fig 3**). The Z_t axis was defined as the line connecting the origin with the proximal end of the tibial tuberosity and approximated the direction of the tibial diaphysis. The Y_t axis was defined as the vector cross product of the Z_t axis and the line connecting the origin and the lateral malleolus and approximated the cranial direction. The X_t axis was defined as the vector cross product of the Y_t and Z_t axes and approximated the lateral direction.

Results

Morphometric data were obtained for 29 muscles (**Table 1**). For most muscles, fiber length was found to

Table 2—Architectural indices of the muscles of the right hind limb in a dog and in humans and cats

	Architectural index		
Muscle	**Dog**	**Humans[14]**	**Cats[15]**
Gluteus superficialis	0.55	NR	NR
Gluteus medius	0.38	NR	NR
Gluteus profundus	0.14	NR	NR
Piriformis	0.35	NR	NR
Tensor fasciae latae, cranial part	0.22	NR	NR
Tensor fasciae latae, caudal part	0.83	NR	NR
Sartorius, cranial part	0.71	0.91	0.73
Sartorius, caudal part	0.75	0.91	0.73
Rectus femoris	0.18	0.21	0.24
Biceps femoris	0.36	0.50	0.38
Abductor cruris caudalis	0.74	NR	NR
Semimembranosus	0.81	0.23	0.83
Semitendinosus	0.68	0.50	0.49
Gracilis	0.66	0.83	0.84
Adductor longus	0.55	0.38	0.64
Adductor magnus et brevis	0.67	0.66	0.90
Pectineus	0.23	0.85	0.75
Obturatorius internus	0.31	NR	NR
Obturatorius externus	0.42	NR	NR
Gemelli	0.28	NR	NR
Quadratus femoris	0.63	NR	NR
Articularis coxae	0.76	NR	NR
Iliopsoas	0.39	NR	NR
Vastus lateralis and intermedius	0.37	0.21	0.28
Vastus medialis	0.22	0.21	0.32
Extensor digitorum longus	0.20	0.23	0.35
Gastrocnemius, medial head	0.12	0.15	0.23
Gastrocnemius, lateral head	0.09	0.23	0.26
Popliteus	0.21	0.26	NR

NR = Not reported.

Table 3—Coordinates of the origins and insertions of the muscles of the right hind limb in a dog

Muscle	X_p	Y_p	Z_p	X_f	Y_f	Z_f	X_t	Y_t	Z_t
Gluteus superficialis	−21.86	54.60	25.64	30.62	−2.10	155.60	NA	NA	NA
Gluteus medius	−6.34	81.44	6.31	23.36	9.42	174.67	NA	NA	NA
Gluteus profundus	−6.35	50.40	5.41	29.32	2.37	167.30	NA	NA	NA
Piriformis	−8.98	29.06	13.36	23.36	9.42	174.67	NA	NA	NA
Tensor fasciae latae, cranial part	3.87	70.83	−14.24	11.50	−18.39	10.65	NA	NA	NA
Tensor fasciae latae, caudal part	3.87	70.83	−14.24	19.04	−4.010	136.87	NA	NA	NA
Sartorius, cranial part	6.98	91.94	−13.25	−0.74	−20.56	−5.50	NA	NA	NA
Sartorius, caudal part	9.20	84.14	−19.09	NA	NA	NA	−7.29	−5.53	165.11
Rectus femoris	3.42	20.22	−2.74	NA	NA	NA	−0.51	−4.25	183.74
Biceps femoris	11.92	−29.97	37.81	NA	NA	NA	7.32	−8.52	187.53
Abductor cruris caudalis	0.72	−20.95	29.49	NA	NA	NA	0.21	−3.87	72.62
Semimembranosus	4.51	−44.80	32.71	−9.00	−3.69	15.16	NA	NA	NA
Semitendinosus	15.19	−33.64	34.02	NA	NA	NA	−8.91	−5.53	150.42
Gracilis	−35.89	−22.93	−12.00	NA	NA	NA	−8.32	−5.41	158.10
Adductor longus	−35.97	−28.10	−4.20	9.07	8.20	127.70	NA	NA	NA
Adductor magnus et brevis	−35.90	−28.10	−4.20	5.67	0.12	84.33	NA	NA	NA
Pectineus	−16.93	1.33	−20.20	2.32	−3.05	70.94	NA	NA	NA
Obturatorius internus	−6.49	−8.33	26.01	13.85	10.40	155.92	NA	NA	NA
Obturatorius externus	1.88	−21.52	23.12	13.85	10.40	155.92	NA	NA	NA
Gemelli	1.88	−21.52	23.12	13.85	10.40	155.92	NA	NA	NA
Quadratus femoris	2.60	−38.30	26.61	8.71	11.77	138.75	NA	NA	NA
Articularis coxae	−1.39	17.89	7.81	−2.42	−0.73	156.31	NA	NA	NA
Iliopsoas	−1.53	33.18	−4.77	−2.34	12.94	146.06	NA	NA	NA
Vastus lateralis and intermedius	NA	NA	NA	17.59	3.56	152.49	−0.39	−1.05	179.72
Vastus medialis	NA	NA	NA	0.48	3.29	145.11	−0.51	−4.25	183.74
Extensor digitorum longus	NA	NA	NA	6.20	−3.74	16.79	−19.52	62.74	−90.40
Gastrocnemius, medial head	NA	NA	NA	−17.70	0.08	0.18	11.86	−27.72	5.16
Gastrocnemius, lateral head	NA	NA	NA	17.48	1.10	−1.79	11.86	−27.72	5.16
Popliteus	NA	NA	NA	13.71	6.42	−12.64	−1.99	−30.46	166.48

All measurements are given in millimeters.
X_p, Y_p, and Z_p = Pelvic bone coordinates. X_f, Y_f, and Z_f = Femoral bone coordinates. X_t, Y_t, and Z_t = Tibial bone coordinates. NA = Not applicable.

Table 4—Coordinates of prominent bony landmarks on the pelvis of a dog

Bony landmark	X_p	Y_p	Z_p
Pubic tubercle	−40.55	−14.08	−23.31
Right cranial dorsal iliac spine	−7.27	91.59	21.41
Left cranial dorsal iliac spine	−74.13	90.25	22.58
Right cranial ventral iliac spine	7.663	84.17	−23.24
Left cranial ventral iliac spine	−88.98	86.00	−23.29
Right caudal dorsal iliac spine	−14.63	55.16	19.08
Left caudal dorsal iliac spine	−68.97	56.66	19.42
Left ischiatic tuberosity	−92.30	−30.83	37.76
Center of left acetabulum	−79.93	0.50	0.57
Center of right acetabulum	0	0	0
Center of sacrum	39.97	73.38	−0.92

See Table 3 for key.

Table 5—Coordinates of prominent bony landmarks on the right femur of a dog

Bony landmark	X_f	Y_f	Z_f
Origin of cranial cruciate ligament	−0.23	7.37	−9.13
Origin of caudal cruciate ligament	−7.20	8.03	−9.72
Center of patella	−1.99	−10.35	−14.67
Center of femoral head	−0.02	0.66	167.67
Center of knee joint	−3.71	6.90	16.79
Midpoint between medial and lateral epicondyles	0	0	0

See Table 3 for key.

Table 6—Coordinates of prominent bony landmarks on the right tibia of a dog

Bony landmark	X_t	Y_t	Z_t
Insertion of cranial cruciate ligament	4.18	−18.99	187.87
Insertion of caudal cruciate ligament	5.25	−35.89	180.73
Lateral malleolus	15.90	0.78	1.05
Medial malleolus	−15.90	−0.78	−1.05
Lateral condyle	24.77	−29.93	178.06
Medial condyle	−15.09	−36.37	184.28
Center of knee joint	4.71	−27.44	184.30
Center of metatarsal pad	−17.14	93.53	−66.92
Midpoint between medial and lateral malleoli	0	0	0

See Table 3 for key.

be uniform. The AI for muscles of this dog were compared with AI reported for humans and cats (**Table 2**). Coordinates of the origins and insertions of these 29 muscles were also determined (**Table 3**), along with coordinates of landmarks on the pelvis (**Table 4**), femur (**Table 5**), and tibia (**Table 6**).

Discussion

In 1981, Dostal and Andrews published a 3-dimensional geometric model of the human hip musculature.[7] These results served as a database for studies that determined hip joint reaction forces and forces in the muscles surrounding the hip during the entire gait cycle.[5,6] They have also been used in a variety of biomechanical investigations of the human lower limb, including calculation of stresses in the femur during 1-legged stance, calculation of the internal forces and moments in the femur during walking, evaluation of the muscle forces involved in the transfer of spinal load to the pelvis and legs, and evaluation of loads transferred across the pelvic bone.[28-33] It is hoped that results of the present study will serve as a similar database for biomechanical studies of the hind limb in dogs.

To our knowledge, only 1 biomechanical analysis of the forces acting around the hip joint in dogs has been published.[34] Authors of that study, however, analyzed a simple 2-dimensional model that considered only 1 muscle, and results, therefore, are relatively inaccurate. The present study was intended to provide a comprehensive database of information required for 3-dimensional biomechanical analyses of the hind limb in dogs. Results of such analyses will help us better understand the physiology of locomotion in dogs and the mechanisms leading to hind limb injury.

The first part of this study involved collection of morphometric data for the muscles of the hind limb. It is difficult to measure muscle forces in vivo because of technical, biological, and ethical problems. Therefore, methods have been developed to estimate them. Most methods used to estimate muscle forces are based on the assumption that a muscle's ability to generate force is in some way related to its size. The exact nature of this relationship is not known; however, the concept of PCSA represents a widely accepted first approximation of this relationship.[6,10,13,20]

The accepted method for calculating PCSA uses the ratio of muscle volume to mean muscle fiber length. This is a very tedious method and is not practical for collection of data from a large number of cadavers.[35] For this reason, most published biomechanical models of the human lower leg used PCSA obtained from the dissection of only 2 or 3 cadavers.[6,14] In the present study, calculations were performed with data from only a single cadaver. However, we believe that these values still provide useful information about the hind limbs of dogs.

For most muscles, the AI (ie, the ratio between muscle fiber length and total muscle length) in this dog was similar to the AI reported for cats and humans.[14,15] Notable exceptions were the semimembranosus muscle, for which the AI in humans was much less than the AI in the dog and in cats, and the pectineus muscle, for which the AI in the dog was much less than the AI in cats and humans. No obvious reasons could be found for these differences, and they were attributed to individual variations in the specimens used.

The physiologic relationship between muscle size and muscle force is poorly understood at this time. For instance, PCSA is used as an estimate of a muscle's ability to generate force, but calculation of the PCSA does not take into account the presence of different fiber types in the muscle. Similarly, angle of pennation is only partly taken into account. The angle of pennation is defined as the angle formed between individual muscle fibers and the line of force exerted by the muscle. The PCSA of a muscle is dependent on this angle; however, the angle of pennation has a significant effect on PCSA only for muscles with angles of pennation > 20°, because the cosine of angles < 20° is > 0.94, and multiplication by this factor does not substantially alter the result.[16] Because all muscles examined in the present study were found to have angles of pennation < 20° and most had angles < 5°, angles of pennation were ignored in the calculation of PCSA in this study.

Brand et al[35] evaluated how sensitive joint force and muscle force predictions were to changes in PCSA. They showed that calculated muscle forces were sensitive to variations in PCSA and, therefore, must be interpreted with caution, allowing for a certain range of error. However, peak joint forces that were calculated were substantially less sensitive to changes in PCSA than were calculated muscle forces.

The second part of the present study involved determining the 3-dimensional coordinates of the origins and insertions of the muscles of the hind limb. These data are required to allow determination of the lines of action and moment arms of the muscles. Coordinates of prominent bony landmarks were also obtained for each of the bones of the hind limb. Transformation of these coordinates allows researchers to determine the coordinates of origin and insertion of each muscle for different orientations of the body segments during the different stages of gait.[36] It will, therefore, be possible to calculate muscle forces during each stage of the gait.

Anatomic data of this model are limited by several possible sources of error. First, the model does not account for marking errors. This is especially true for muscles with a large area of insertion or origin, such as the gluteus medius muscle. The importance of this source of error has been previously estimated, and although it can be considerable, the effect on most moment arm calculations was found to be minor.[10] Another potential source of error is the large differences in muscle origins and insertions among dogs of different breeds and even among dogs of the same breed. The coordinates of the origins and insertions of the various muscles were obtained from measurements in a particular skeleton. Therefore, data from this specimen cannot be used for other dogs without some form of anthropometric scaling. Homogeneous and nonhomogeneous anthropometric scaling methods have been described for human and canine bones.[26,27,35]

[a]Coordinate measuring machine-B231, Mitutoyo Corp, Kawasaki, 213 Japan.

References

1. Seireg A, Arvikar RJ. A mathematical model for evaluation of forces in lower extremities of the musculo-skeletal system. *J Biomech* 1973;6:313–326.

2. Seireg A, Arvikar RJ. The prediction of muscular load sharing and joint forces in the lower extremities during walking. *J Biomech* 1975;8:89–102.

3. Ghista DN, Toridis TG, Srinivasan TM. Human gait analysis: determination of instantaneous joint reactive forces, muscle forces and the stress distribution in bone segments. Part I. *Biomed Tech (Berl)* 1975;20:204–213.

4. Ghista DN, Toridis TG, Srinivasan TM. Human gait analysis: determination of instantaneous joint reactive forces, muscle forces and the stress distribution in bone segments. Part II. *Biomed Tech (Berl)* 1975;21:66–74.

5. Crowninshield RD, Johnston RC, Andrews JG, et al. A biomechanical investigation of the human hip. *J Biomech* 1978;11:75–85.

6. Crowninshield RD, Brand RA. A physiologically based criterion of muscle force prediction in locomotion. *J Biomech* 1981;14:793–801.

7. Dostal WF, Andrews JG. A three dimensional biomechanical model of hip musculature. *J Biomech* 1981;14:803–812.

8. Patriarco AG, Mann RW, Simon SR, et al. An evaluation of the approaches of optimization models in the prediction of muscle forces during human gait. *J Biomech* 1981;14:513–525.

9. Brand RA, Crowninshield RD, Wittstock CE, et al. A model of lower extremity muscular anatomy. *J Biomech Eng* 1982;104:304–310.

10. An KN, Chao EYS, Kaufman KR. Analysis of muscle and joint loads. In: Mow VC, Hayes WC, eds. *Basic orthopedic biomechanics*. 2nd ed. Philadelphia: Lippincott-Raven, 1997;1–35.

11. Hardt DE. Determining muscle forces in the leg during normal human walking—an application and evaluation of optimization methods. *J Biomech Eng* 1978;100:72–78.

12. Crowninshield RD. Use of optimization techniques to predict muscle forces. *J Biomech Eng* 1978;100:88–92.

13. Kaufman KR, An KN, Litchy WJ, et al. Physiological prediction of muscle forces—I. Theoretical formulation. *Neuroscience* 1991;40:781–792.

14. Wickiewicz TL, Roy RR, Powell PL, et al. Muscle architecture of the human lower limb. *Clin Orthop* 1983;179:275–283.

15. Sacks RD, Roy RR. Architecture of the hind limb muscles of cats: functional significance. *J Morphol* 1982;173:185–195.

16. Thorpe SKS, Crompton RH, et al. Dimensions and moment arms of the hind- and forelimb muscles of common chimpanzees (*Pan troglodytes*). *Am J Phys Anthropol* 1999;110:179–199.

17. Jensen RH, Davy DT. An investigation of muscle lines of action about the hip: centroid line approach vs. the straight line approach. *J Biomech* 1975;8:103–110.

18. Herzog W, Read LJ. Lines of action and moment arms of the major force-carrying structures crossing the human knee joint. *J Anat* 1993;182:213–230.

19. Johnson GR, Spalding D, Nowitzke A, et al. Modeling the muscles of the scapula; morphometric and coordinate data and functional implications. *J Biomech* 1996;29:1039–1051.

20. Raikova R. About weight factors in the non-linear objective functions used for solving indeterminate problems in biomechanics. *J Biomech* 1999;32:689–694.

21. Mendes J, Keys A. Density and composition of mammalian muscle. *Metabolism* 1960;9:184–188.

22. Evans HE, Christensen GC. *Miller's anatomy of the dog*. Philadelphia: WB Saunders Co, 1979;374–410.

23. Adrian MJ, Roy WE, Karpovich PV. Normal gait of the dog: an electrogoniometric study. *Am J Vet Res* 1966;27:90–95.

24. Mann FA, Wagner-Mann C, Tangner DH. Manual goniometric measurement of the canine pelvic limb. *J Am Anim Hosp Assoc* 1988;24:189–194.

25. Pedersen DR, Feinberg JH, Brand RA. A model to predict canine pelvic limb musculoskeletal geometry. *Acta Anat (Basel)* 1991;140:139–145.

26. Lewis JL, Lew WD, Zimmerman JR. A nonhomogeneous anthropometric scaling method based on finite element principles. *J Biomech* 1980;13:815–824.

27. Lew WD, Lewis JL. An anthropometric scaling method with application to the knee joint. *J Biomech* 1977;10:171–181.

28. Dalstra M, Huiskes R. Load transfer across the pelvic bone. *J Biomech* 1995;28:715–724.

29. Cristofolini L, Viceconti M, Toni A, et al. Influence of thigh muscles on the axial strains in a proximal femur during early stance in gait. *J Biomech* 1995;28:617–624.

30. Taylor ME, Tanner KE, Freeman MAR, et al. Stress and strain distribution within the intact femur: compression or bending? *Med Eng Phys* 1996;18:122–131.

31. Duda GN, Schneider E, Chao EYS. Internal forces and moments in the femur during walking. *J Biomech* 1997;30:933–941.

32. Hoek van Dijke GA, Snijders CJ, Stoeckart R, et al. A biomechanical model on muscle forces in the transfer of spinal load to the pelvis and legs. *J Biomech* 1999;32:927–933.

33. Gracovetsky S, Farfan HF, Lamy C. A mathematical model of the lumbar spine using an optimized system to control muscles and ligaments. *Orthop Clin North Am* 1977;8:135–153.

34. Arnoczky SP, Torzilli PA. Biomechanical analysis of forces acting about the canine hip. *Am J Vet Res* 1981;42:1581–1585.

35. Brand RA, Pedersen DR, Friederich JA. The sensitivity of muscle force predictions to changes in physiologic cross-sectional area. *J Biomech* 1986;19:589–596.

36. Grood ES, Suntay WJ. A joint coordinate system for the clinical description of three-dimensional motions: Application to the knee. *J Biomech Eng* 1983;105:136–144.